BIOCHEMISTRY
including biophysical chemistry & molecular biology
Article

Biochemistry **2010,** *49,* 6115–6121 6115
DOI: 10.1021/bi100492p

Delineating Electrogenic Reactions during Lactose/H^+ Symport†

Juan J. Garcia-Celma,‡ Julian Ploch,‡ Irina Smirnova,§ H. Ronald Kaback,*,§,∥,⊥ and Klaus Fendler*,‡

‡*Department of Biophysical Chemistry, Max-Planck-Institute of Biophysics, D-60438 Frankfurt/M, Germany,* §*Department of Physiology,* ∥*Department of Microbiology and Immunology, and* ⊥*Department of Molecular Genetics, University of California, Los Angeles, California 90095-7327*

Received April 1, 2010; Revised Manuscript Received June 17, 2010

ABSTRACT: Electrogenic reactions accompanying downhill lactose/H^+ symport catalyzed by the lactose permease of *Escherichia coli* (LacY) have been assessed using solid-supported membrane-based electrophysiology with improved time resolution. Rates of charge translocation generated by purified LacY reconstituted into proteoliposomes were analyzed over a pH range from 5.2 to 8.5, which allows characterization of two electrogenic steps in the transport mechanism: (i) a weak electrogenic reaction triggered by sugar binding and observed under conditions where H^+ translocation is abolished either by acidic pH or by a Glu325 → Ala mutation in the H^+ binding site (this step with a rate constant of ~200 s^{-1} for wild-type LacY leads to an intermediate proposed to represent an "occluded" state) and (ii) a major electrogenic reaction corresponding to 94% of the total charge translocated at pH 8, which is pH-dependent with a maximum rate of ~30 s^{-1} and a p*K* of 7.5. This partial reaction is assigned to rate-limiting H^+ release on the cytoplasmic side of LacY during turnover. These findings together with previous electrophysiological results and biochemical−biophysical studies are included in an overall kinetic mechanism that allows delineation of the electrogenic steps in the reaction pathway.

The lactose permease of *Escherichia coli* (LacY)[1] is a galactopyranoside/H^+ symporter that belongs to the major facilitator superfamily (MFS) of membrane transport proteins (*1*, *2*). LacY is arguably the most thoroughly studied ion-coupled membrane transport protein (*3*−*7*). X-ray crystal structures exhibit an inward-open conformation with a tightly packed, closed periplasmic side and a large hydrophilic cavity open only to the cytoplasm with sugar- and H^+-binding sites in the middle of the molecule at the apex of the hydrophilic cavity. Although an outward-open conformation has not yet been obtained by X-ray crystallography, it is well documented that LacY undergoes conformational changes upon sugar binding that lead to closing of the cytoplasmic cavity and opening of a relatively large hydrophilic cavity on the periplasmic side (the alternating access model). Therefore, estimates of distance from cross-linking measurements in the inward-facing structure (*3*), site-directed alkylation (*8*−*11*), single-molecule Förster resonance energy transfer (*12*), double electron−electron resonance (*13*), site-directed thiol cross-linking (*14*), and site-directed quenching and unquenching of Trp fluorescence (*15*) all provide strong, independent support for the alternating access model.

For a detailed investigation of the alternating access model, resolution of the partial reactions in the transport cycle is essential. This requires a method with sufficient time resolution such as solid-supported membrane (SSM)-based electrophysiology (*16*, *17*), which allows concentration jumps as rapid as 4.5 ms (*17*). This fast solution exchange in combination with quantitative temporal information concerning the surface substrate concentration rise time is utilized to detect rapid charge displacements in the reaction cycle of LacY and to determine rate constants. A kinetic model for sugar transport in LacY is presented, and a transport mechanism including an occluded state is proposed.

EXPERIMENTAL PROCEDURES

Construction of Mutants and LacY Purification. Construction of mutants and purification of the His-tagged proteins were conducted as described previously (*13*). Purified proteins (10−15 mg/mL) in a 50 mM sodium phosphate/0.01% DDM (pH 7.5) mixture were frozen in liquid nitrogen and stored at −80 °C until they were used.

Reconstitution of Proteoliposomes. Reconstitution of the purified wild type or E325A mutant was conducted with *E. coli* total phospholipids (Avanti Polar Lipids, Alabaster, AL) by using octyl glucoside dilution, followed by one cycle of freeze−thaw sonication (*18*, *19*). Purified wild-type LacY or the E325A mutant and liposomes were mixed at a lipid:protein ratio of 5 (weight/weight), as indicated. Prior to use, the samples were thawed on ice and gently sonicated for 2−5 s.

SSM-Based Electrophysiology. SSM measurements were performed as described previously (*16*, *17*, *20*−*22*). Briefly, 40 μL of proteoliposomes at a protein concentration of 1 mg/mL was allowed to adsorb for 1 h to an octadecanethiol/diphytanoylphosphatidylcholine hybrid bilayer on a gold surface of the sensor. The solution exchange protocol consisted of three phases: (1) nonactivating solution (2 s), (2) activating solution (2 s), and (3) nonactivating solution (2 s). A valveless diverter fluidic geometry

†This work was funded by the Deutsche Forschungsgemeinschaft SFB 807 (to K.F.) and by National Institutes of Health Grants DK051131, DK069463, GM073210, and GM074929 and National Science Foundation Grant 0450970 to H.R.K.

*To whom correspondence should be addressed. K.F.: e-mail, klaus.fendler@biophys.mpg.de; phone, +49-69-63032035; fax, +49-69-63032222. H.R.K.: e-mail, rkaback@mednet.ucla.edu; phone, (310) 206-5053; fax, (310) 206-8623.

[1]Abbreviations: LacY, lactose permease; MelB, melibiose permease; SSM, solid-supported membrane; DTT, dithiothreitol; MFS, major facilitator superfamily; SE, standard error.

Published on Web 06/22/2010

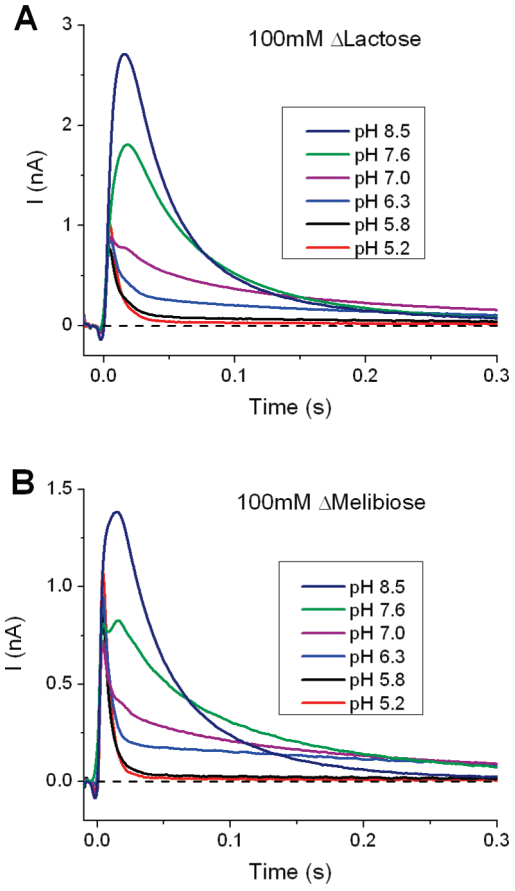

FIGURE 1: Transient currents measured with wild-type LacY proteoliposomes after 100 mM lactose (A) or melibiose (B) concentration jumps at different pH values as indicated. Nonactivating solutions contained 100 mM glucose while activating solutions 100 mM lactose (A) or melibiose (B). All solutions where prepared in 100 mM potassium phosphate buffer at the indicated pH with 1 mM DTT. All traces were recorded at the same sensor. $t = 0$ corresponds to the time at which the activating solution reaches the sensor surface.

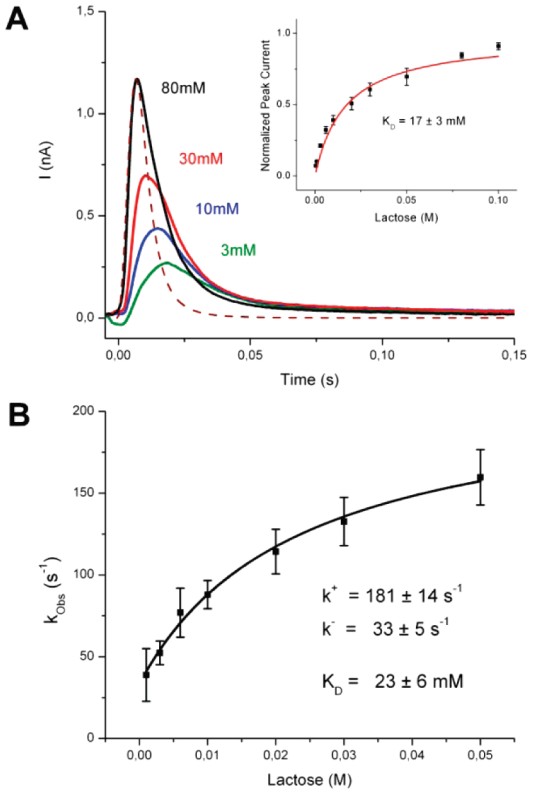

FIGURE 2: (A) Transient currents measured for wild-type LacY proteoliposomes after different lactose concentration jumps as indicated at pH 5.2. Nonactivating solutions contained 100 mM glucose and activating solutions a concentration of x mM lactose with $100 - x$ mM glucose to maintain a constant sugar concentration. Solutions were prepared in 100 mM potassium phosphate buffer (pH 5.2) with 1 mM DTT. All traces were recorded at the same sensor. $t = 0$ corresponds to the time at which the activating solution reaches the sensor surface. The transfer function of the experiment representing the time resolution is shown as a dashed line. The inset shows the dependence of the peak currents on lactose concentration. Average normalized peak currents and SE are given. An apparent K_D of 17 ± 3 mM is obtained from the hyperbolic fit (red trace). (B) Rate constants determined from the transient currents at different lactose concentrations at pH 5.2. From the transient currents, the rate constants were calculated with an iterative least-squares deconvolution algorithm (*17*, *22*). Average rate constants and SE from three or four data sets at a given lactose concentration are given. A hyperbolic fit to the data yields values for the forward ($k_2^+ = 181 \pm 14\ s^{-1}$) and reverse ($k_2^- = 33 \pm 5\ s^{-1}$) rate constants, as well as for the apparent K_D (23 ± 6 mM) (see eq 2).

was chosen to apply the different solutions (*22*) at a flow rate of 0.46 mL/s. The nonactivating solution always contained 100 mM glucose, and the activating solution contained lactose or melibiose at a concentration of 100 mM, unless stated otherwise (Figure 2). All solutions were buffered in 100 mM potassium phosphate buffer at a given pH value with 1 mM dithiothreitol (DTT). Currents were recorded throughout the entire time using a current amplifier set to a gain of 10^9−10^8 V/A and a rise time (10−90%) of 3 ms.

RESULTS

Reduced Downhill Sugar/H^+ Symport by Wild-Type LacY at Low pH. Proteoliposomes reconstituted with purified wild-type LacY were immobilized on an SSM-coated gold electrode (the sensor) as described previously (*17*). The transient currents generated after sugar concentration jumps were recorded at an improved time resolution [8 ms as compared to 15 ms (*17*)], and the effect of pH was investigated over a wide range from pH 5.2 to 8.5 (Figure 1A,B). Because all traces were recorded on the same sensor, the amplitudes are directly comparable. To equilibrate the pH across the proteoliposome membrane after the pH of the solutions had been changed, the immobilized proteoliposomes were incubated for several minutes at the new pH. Subsequent substrate concentration jumps produced constant currents indicating that the pH value in the proteoliposomes had indeed adjusted to the external pH.

The current traces fall into three different classes (Figure 1A). (1) At alkaline pH (7.6 and 8.5 for lactose), the magnitudes of the signals decrease with a decay time from peak to half-maximal current ($\tau_{1/2}$) of more than 20 ms. These transient currents are dominated by steady-state electrogenic downhill sugar/H^+ symport, and their decay is due to charging of the liposomal membrane by the transport activity of LacY (*17*). In this pH range, the peak currents recorded with lactose are larger than with melibiose, in agreement with lactose being the substrate transported with the highest turnover (*17*). (2) At intermediate pH values (7.0 and 6.3 for lactose), the transient currents are clearly biphasic. The improvement in time resolution allows resolution of a double peak (pH 7.0 for lactose). This double peak is even more pronounced with a 100 mM melibiose concentration jump at pH 7.6. A double peak can only be explained

with at least two electrogenic steps in the reaction cycle. At pH 6.3, the double peak disappears (for lactose), but a second slowly decaying component is still observed. This type of biphasic decay was previously observed for the melibiose permease (MelB) from *E. coli* (*21*), where the rapid transient is associated with an electrogenic conformational transition triggered by melibiose binding, and the second slow phase represents the electrogenic transport activity of the symporter. (3) For lactose concentration jumps at pH < 6.3, the first peak becomes the major component of the transient currents. The current transients are similar to those recorded with the mutants defective in transport (*17*; see below), which indicates that these signals are due to rapid charge displacements induced by sugar binding (*17*) in the absence of significant transport activity of LacY (*23*, *24*). A similar pattern of three different classes of transient currents is observed with melibiose concentration jumps (Figure 1B).

Initial Charge Displacements in Wild-Type LacY. At pH 5.2, the electrogenic response of wild-type LacY is almost exclusively a fast initial charge displacement (Figure 1A,B). To further characterize this initial charge displacement, the transient currents of wild-type LacY after lactose concentration jumps were investigated in more detail (Figure 2). An increase in the lactose concentration results in an increase in the peak current of the initial charge displacement. In addition, the position of the peak and the width of the transients depend on the substrate concentration. For statistical analysis, the concentration dependence of the peak current was measured in four data sets. Hyperbolic fits to each of the four individual data sets yielded saturation values I_{Max}. For a direct comparison between different data sets, the peak currents of each data set were normalized to their corresponding I_{Max}. Average normalized peak currents and standard errors (SE) are shown in the inset of Figure 2A. From the hyperbolic fit to the averaged peak currents, an apparent K_D of 17 ± 3 mM is obtained. For comparison, a K_D for lactose of 1−2 mM was previously measured at 4 °C in right-side-out or inside-out membrane vesicles by protection of a single Cys148 against alkylation (*25*).

Determination of Rate Constants. As shown in Figure 2A, the time constants of the transient currents depend on the substrate concentration. To recover the rate constants of the current generated by the symporter, the time resolution of the experiments must be taken into account. In the measurements presented here, the time resolution was determined to be 8 ms using a ClO_4^- concentration jump and the SSM as described previously (*22*). The corresponding transfer function is given for comparison with the transient currents in Figure 2A (dashed line). The rate constants of the observed charge displacements were derived from the transient currents as described previously (*22*) and in the Supporting Information of ref *17*. The hyperbolic dependence of the rate constants on the substrate concentration is expected for a two-step reversible binding mechanism in which the first step is electroneutral and the second electrogenic. This two-step reversible reaction can be described as follows:

$$E + S \overset{K_D}{\leftrightarrow} ES \underset{k^-}{\overset{k^+}{\leftrightarrow}} ES* \qquad (1)$$

The first step represents electroneutral binding of the substrate S to the enzyme E with a substrate dissociation constant K_D. The second step is electrogenic and characterized by forward (k^+) and reverse (k^-) rate constants. Assuming rapid substrate binding, the observed rate constant (k_{obs}) shows a hyperbolic dependence

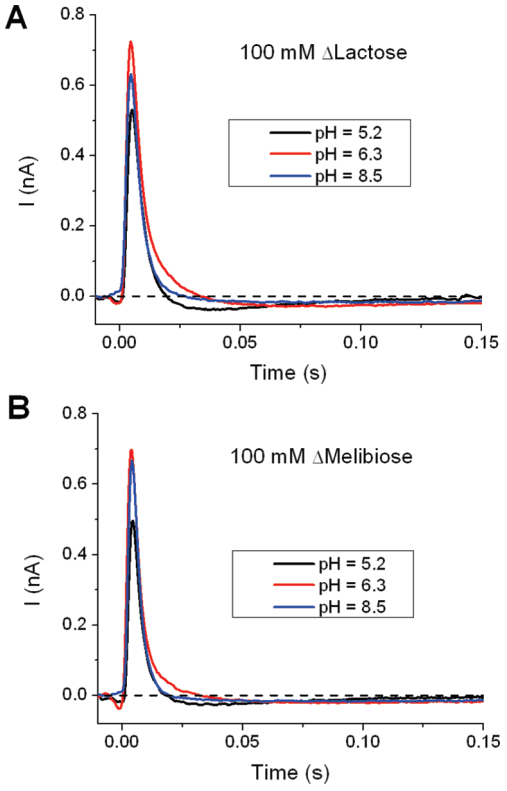

FIGURE 3: Transient currents measured with E325A LacY proteoliposomes after 100 mM lactose (A) or melibiose (B) concentration jumps at different pH values as indicated. The solution composition and flow protocol are the same as those described in the legend of Figure 1. All traces were recorded at the same sensor. $t = 0$ corresponds to the time at which the activating solution reaches the sensor surface.

on the substrate concentration [S] (*26*):

$$k_{obs} = k^- + k^+ \frac{[S]}{[S] + K_D} \qquad (2)$$

A hyperbolic fit of the observed rate constants gives the values for the forward ($k^+ = 181 \pm 14\ s^{-1}$) and reverse ($k^- = 33 \pm 5\ s^{-1}$) rate constants of the electrogenic partial reaction, as well as for the K_D. Notably, the value obtained for the K_D from analysis of the observed rate constants ($K_D = 23 \pm 6$ mM) is in good agreement with the value obtained from the analysis of the peak currents.

pH Dependence of E325A LacY. In E325A LacY, all steps involving H^+ translocation are blocked; however, equilibrium lactose exchange and counterflow are intact, and the binding affinity is independent of pH and equal to the wild-type affinity over the physiological pH range (*23*, *24*, *27*). Proteoliposomes reconstituted with purified E325A LacY were immobilized on an SSM sensor and activated with 100 mM concentration jumps of lactose or melibiose at given pH values (Figure 3). In marked contrast to those with wild-type LacY, the transient currents observed with the mutant have almost identical shape and only slightly varying amplitudes over the entire pH range investigated from pH 5.2 to 8.5. These findings suggest that the particular electrogenic reaction observed in the mutant does not result from a protonation or deprotonation event. With E325A LacY, similar transient currents are observed with both lactose and melibiose at all investigated pH values (panels A and B of Figure 3, respectively). These characteristics indicate that the same charge is displaced during lactose or melibiose binding.

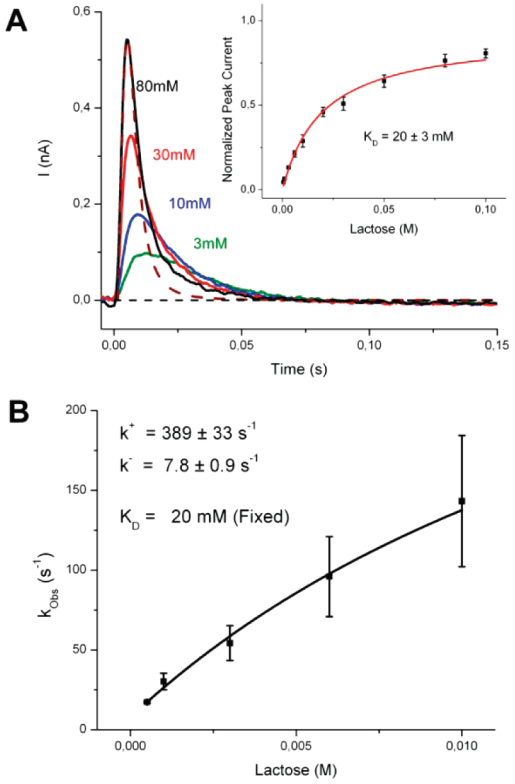

FIGURE 4: Transient currents measured with E325A LacY proteoliposomes after different lactose concentration jumps as indicated at pH 7.0. Except for the pH, the solution composition and flow protocol are the same as those used for Figure 2. All traces were recorded at the same sensor. $t = 0$ corresponds to the time at which the activating solution reaches the sensor surface. The transfer function of the experiment representing the time resolution is shown as a dashed line. The inset shows the dependence of the peak currents on the lactose concentration. Average normalized peak currents and SE are given. An apparent K_D of 20 ± 3 mM is obtained from the hyperbolic fit (red trace). (B) Rate constants determined from the transient currents at different lactose concentrations at pH 7.0. From the transient currents, the rate constants were calculated with an iterative least-squares deconvolution algorithm (*17*, *22*). Average rate constants and SE from three data sets at a given lactose concentration are given. A hyperbolic fit to the data yields values for the forward ($k_2^+ = 389 \pm 33\ s^{-1}$) and reverse ($k_2^- = 7.8 \pm 0.9\ s^{-1}$) rate constants. The fit was obtained with a fixed K_D of 20 mM (see eq 2).

At the same time, the corresponding partial reactions are probably too fast to be resolved ($k > 200\ s^{-1}$) and the time dependence of the transient currents is limited by the time resolution of the technique.

With both substrates at all pH values, the signals also display a small slow negative phase. This behavior is characteristic for the capacitively coupled system and indicates the absence of LacY symport activity (*16*), which is consistent with biochemical data (*23*, *24*). Similar behavior has been found for NaK-ATPase under conditions of reduced steady-state transport (*28*).

Because mutant E325A is fully functional with respect to sugar binding, the same kinetic model (eqs 1 and 2) was used for the determination of the rate constants as for the wild type. However, it is clear from Figure 4A that the currents decay faster than in the wild type, which complicates the analysis. At lactose concentrations of >10 mM, the transfer function (Figure 4A, dashed line) nearly coincides with the current traces, indicating that the time resolution of the SSM measurements is no longer sufficient for the determination of rate constants. Therefore, rate constants were determined up to a lactose concentration of only 10 mM (Figure 4B). Under these circumstances, the forward rate constant (k^+) can be determined only if a reliable estimate for the dissociation constant (K_D) is available. We have used a K_D of 20 mM, as determined from the rates of wild-type LacY (Figure 2B), because it is well documented that the sugar binding affinities of mutant E325A and wild-type LacY are similar (*27*). To determine the rate constants for the E325A mutant ($k^+ = 389 \pm 33\ s^{-1}$, and $k^- = 7.8 \pm 0.9\ s^{-1}$), data were fitted using this fixed K_D. This result should be taken with caution, as the possibility that the saturation observed for the peak currents with the mutant is due to limited time resolution cannot be excluded. Thus, the K_D determined and the forward rate constant (k^+) represent only lower limits for these constants.

DISCUSSION

A Four-State Kinetic Model with Two Electrogenic Steps Describes Quantitatively the pH Dependence of the Transient Current. On the basis of the comparison of wild-type LacY with two symport impaired mutants, E325A and C154G, it was suggested (*17*) that turnover of LacY involves two electrogenic steps at pH 7.6: (i) a minor electrogenic step triggered by sugar binding (representing only 6% of the charge translocated by wild-type LacY) and (ii) a major electrogenic step due probably to cytoplasmic H^+ release. Now we have resolved the sugar-induced minor electrogenic charge displacement in the wild-type symporter as well. For this purpose, wild-type LacY was investigated using a better time resolution and over a broader pH range. At acidic pH, the extent of turnover is drastically reduced (*29*−*31*), and signals are observed that are comparable to the transport impaired mutants. Furthermore, at intermediate pH, a signal with two maxima is resolved, which allows the important conclusion that the reaction cycle of LacY contains at least two electrogenic steps.

For the kinetic analysis of the currents at different pH values, a minimal kinetic model was chosen and solved numerically (Figure 5C, inset). The experimental data together with computed transient currents at different pH values are shown in panels A and B of Figure 5. The kinetic model consists of only four intermediates (A, B, C, and D) and four rate constants chosen as follows. (1) The first partial reaction (A → B) is electroneutral, and the rate constant k_1 includes all steps leading to the formation of state B and preceding the minor electrogenic step. This also includes the limited rise time of the substrate concentration at the surface of the SSM defining the time resolution of the experiment. Formation of state B controls the rise time of the transient currents. A value for k_1 of 400 s^{-1} was chosen by manual adjustment of the rising phase of the simulated current traces to the experimental data. (2) The second partial reaction (B → C) corresponds to the minor electrogenic step triggered by sugar binding. As determined previously (*17*) at pH 7.6, a translocated charge of 6% of the total charge translocated by wild-type LacY was assigned to this step. A rate constant k_2 of 200 s^{-1} was taken from the data in Figure 2 and is in agreement with previous measurements (*17*). (3) The third partial reaction (C → D) is electroneutral. An electroneutral partial reaction separating the two electrogenic steps is obligatory to reproduce the signals with two maxima at intermediate pH. A value for k_3 of 250 s^{-1} was chosen by manual adjustment of the simulated current traces to the experimental data. (4) The fourth partial reaction (D → A) is rate-limiting for turnover and corresponds to the major electrogenic step, which displaces the remaining 94% of the total translocated charge per turnover. Because of its promi-

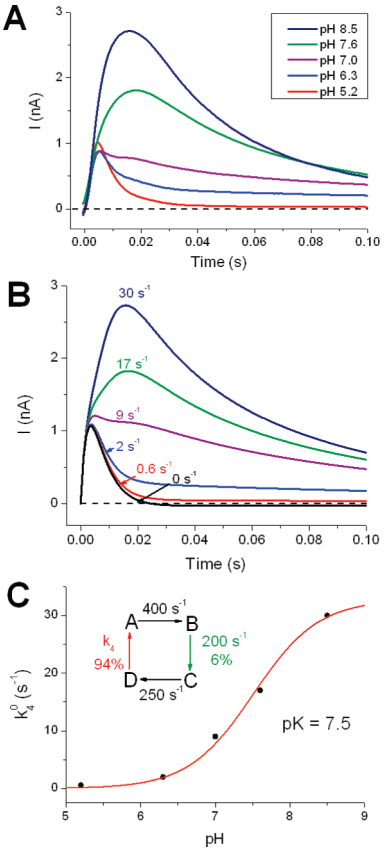

FIGURE 5: Simulation of the transient currents with a four-state kinetic model. (A) Experimental data. For a better comparison between the experimental transient currents and the four-state kinetic model, the experimental transients of Figure 1A (100 mM lactose concentration jumps at different pH values) are represented on an expanded time scale. (B) Numerical solution of the four-state model. The color code for different pH values is given in panel A and applies to both panels. (C) pH dependence of k_4^0 (rate constant k_4 at potential 0). The kinetic model with rate constants is shown in the inset. Partial reactions colored black are electroneutral. The minor electrogenic reaction (6% of the total translocated charge per turnover) is colored green, and the major electrogenic partial reaction (94% of the total translocated charge per turnover) is colored red. The rate constant k_4^0 of the major electrogenic partial reaction takes the values given in the figure at the individual traces (B). A detailed description of the model is given in the text.

nent electrogenicity, the voltage dependence of k_4 is taken into account (note that the voltage dependence of the weakly electrogenic B → C reaction is neglected). In response to the potential generated by the continuous transport activity of LacY, the voltage dependence of k_4 leads to a decay of the currents at >20 ms (Figure 5A), which is taken into account in the model. The kinetic parameter characterizing this partial reaction is its rate constant at zero voltage (k_4^0) which was obtained by manual adjustment of the model to the experimental current traces. As discussed below, this partial reaction corresponds to cytoplasmic H^+ release and is pH-dependent. For each of the current traces measured at different pH values, a given rate constant (k_4^0) was determined (Figure 5B).

The model reproduces the electrogenic response of the symporter from pH 5.2 to 8.5 remarkably well. Notably, all parameters were kept constant, and only k_4^0 was varied. Moreover, the model explains the major features of electrogenic transport at different pH values. (i) At alkaline pH (7.6 and 8.5), the transients decay with a $\tau_{1/2}$ of >20 ms and the magnitude of the peak current decreases at the lower pH value. (ii) At pH 7.0, two maxima are apparent. (iii) At pH 6.3, biphasic behavior is obtained, and the initial charge displacement is observed. The agreement between the model and the experimental findings gives further support to the proposal that two electrogenic steps with very different electrogenicities are involved in the turnover of wild-type LacY.

Using the rate constants k_4^0 at different pH values, a binding curve for a single titratable acidic group with a pK of 7.5 is obtained (Figure 5C). This agrees well with the pH dependence of lactose efflux measured with proteoliposomes reconstituted with purified LacY, where a functional group or proton binding site with a pK of 8.3 must be deprotonated for LacY to catalyze efflux at maximum rates (*31*).

In conclusion, the four-state kinetic model is able to make correct predictions for the measured currents under a variety of different conditions. But most importantly, the kinetic model is minimal in the sense that it contains the fewest partial reactions needed to reproduce the experimental findings. Therefore, the model delineates a unique sequence of partial reactions with the individual rate constants and electrogenicities.

Wild-Type and Mutant E325A. The mutant E325A is specifically defective in all steps involving H^+ release but catalyzes exchange and counterflow at least as well as the wild type (*23*, *24*). Moreover, both the wild type and the mutant have a similar K_D of ~20 mM for lactose binding. Kinetic differences are found for the second reaction of the two-step binding model (eq 1). Sugar binding is approximately twice as fast in the mutant ($k^+ \sim 400\ s^{-1}$) as in the wild type ($k^+ \sim 200\ s^{-1}$). We can further characterize the ES → ES* step with a stability constant ($K_s = k^+/k^-$), which is 50 for the mutant and only 5.5 for the wild type, indicating an ~10-fold shift in the distribution toward ES* in the mutant. On the other hand, the rate constant for another transport impaired mutant, C154G LacY, was considerably smaller ($53 \pm 5\ s^{-1}$) than that of the wild type (*17*).

The four-state kinetic model can also be used for the mutant E325A. As the D → A step in the kinetic model represents deprotonation of LacY, a k_4 of $0\ s^{-1}$ should yield the transient currents for mutant E325A. Indeed, the transient current predicted by the model, assuming $k_4 = 0\ s^{-1}$, consists of an initial charge displacement followed by a slow negative component, in agreement with the measured transients (Figure 3A,B). As the only pH-dependent step in the four-state model is the fourth partial reaction, the model predicts no variation of the transient currents with pH for E325A LacY, which also agrees with the experimental findings (Figure 3A,B).

LacY Transport Mechanism. On the basis of the previous discussion, it is apparent that two electrogenic steps in the LacY reaction cycle can be detected: a rapid sugar-induced initial charge translocation with low electrogenicity and a major electrogenic transition late in the reaction cycle. The latter is also the rate-limiting step in downhill sugar/H^+ symport (*31*) and has been assigned to cytoplasmic H^+ release (*29*), but what is responsible for the minor initial charge displacement?

As LacY before addition of the sugar is in a conformation facing the inside of the proteoliposomes (*3*, *32*−*34*), the question of whether reorientation of the transporter from the inward-facing conformation to the outward-facing conformation can cause the minor charge displacement arises. In this case, if reorientation of LacY is an electrogenic equilibrium followed by fast electroneutral sugar binding, the observed rate would decrease hyperbolically with substrate concentration, in opposition to the experimental results (Figure 2B). This observation

suggests that reorientation of LacY prior to sugar binding does not correspond to the minor electrogenic reaction. The same argument also applies for periplasmic proton binding, the other step in the reaction cycle that takes place before sugar binding. In this case, the mutant E325A which is permanently protonated (*23*, *24*, *27*, *35*) should not be able to generate an electrical response, again in opposition to the experimental results. Alternatively, electrogenic sugar binding to LacY may be responsible for this electrogenic reaction. In this case, however, the observed rate constant would be linearly dependent on the substrate concentration, also opposed to the experimental results. Thus, we propose that sugar binding to LacY triggers an electrogenic partial reaction that takes place in the reaction cycle after sugar binding (eq 1). In this scenario, the observed rate constants hyperbolically increase with substrate concentration (see eq 2), as observed experimentally.

To further define the sugar-induced electrogenic reaction, consideration of the LacY C154G mutant is helpful. In contrast to E325A LacY, mutant C154G is strongly impaired in equilibrium lactose exchange (*36*, *37*). However, C154G LacY binds sugar substrates in a two-step process (*26*), which suggests that after sugar binding C154G LacY forms an intermediate that is unable to release sugar to the cytoplasm, possibly an occluded state. Interestingly, the C154G mutant also displays a sugar-induced electrogenic conformational transition similar to that observed with wild-type LacY at pH 5.2 (Figure 2) and E325A LacY (*17*). Therefore, it seems reasonable to propose that sugar binding also triggers an electrogenic partial reaction in wild-type and E325A LacY leading to formation of an occluded state as proposed previously (*13*).

A reaction cycle for lactose/H^+ symport is shown in Figure 6. It has been suggested that in the absence of sugar LacY is oriented in the membrane in an inward-facing conformation and deprotonated (*17*). From the kinetic analysis presented, it is apparent that LacY binds sugar with a rate constant of at least 400 s^{-1} (see the model in Figure 5C, inset, and the assignment of rate constants at the beginning of the discussion) followed by a weakly electrogenic step ($C_{out}H^+Lac \rightarrow C_{occ}H^+Lac$). We propose that this corresponds to the formation of an intermediate "occluded" state from the outward-facing tertiary complex. In this reaction, only 6% of the total translocated charge is displaced per turnover. The rate constants ($k^+ \sim 180\ s^{-1}$, and $k^- \sim 30\ s^{-1}$) are taken from the analysis of the transient currents shown in Figure 2. Release of sugar ($C_{occ}H^+Lac \rightarrow C_{in}H^+$) is electroneutral and also rapid, proceeding with a rate constant of ~250 s^{-1} (see the parameters of the kinetic model in Figure 5). The rate-limiting process is H^+ release ($C_{in}H^+ \rightarrow C_{in}$), which is also the major electrogenic step with 94% of the total translocated charge. The rate constant varies with pH; at alkaline pH, assuming a value of 30 s^{-1} at alkaline pH. The process has an apparent p*K* of 7.5.

In Figure 6, minor and major electrogenic steps are illustrated by a shallow periplasmic and by a deep cytoplasmic H^+ binding site. However, H^+ displacement through the protein dielectric is only one of several alternative sources of charge displacement such as tilting of helices or movement of charged residues during the transport reaction. It is possible that the sugar-induced minor charge translocation (green arrows in Figure 6) is due to an electrogenic conformational transition not involving the transported cation which was suggested for the melibiose permease (MelB) (*38*).

Indeed, MelB appears to be related to LacY (*39*), although they belong to different families (melB to the glycoside-pentoside-hexuronide:cation symporter and LacY to the MFS family).

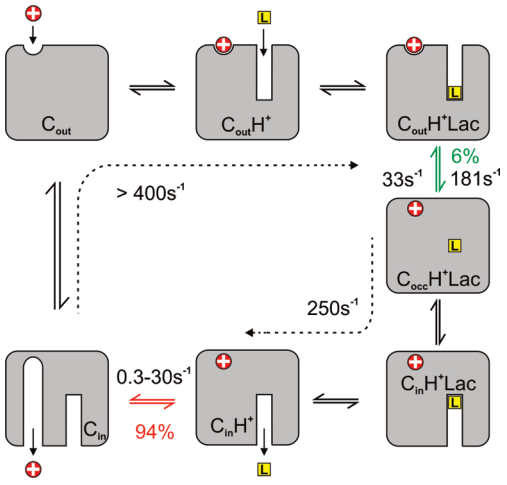

FIGURE 6: Schematic representation of two proposed electrogenic steps in the reaction cycle of wild-type LacY. Inward-facing, outward-facing, and occluded conformations are marked with subscripts in, out, and occ, respectively. L in yellow squares represents the sugar (lactose or melibiose), and red circles with a white cross represent H^+. Addition of sugar leads to a rapid sugar binding ($C_{out}H^+Lac$) with an estimated lower limit for the rate of ~400 s^{-1} (see the text). Sugar binding is followed by a formation of the occluded state ($C_{occ}H^+Lac$) and is accompanied by a minor electrogenic reaction (green) with forward and reverse rate constants of 181 and 33 s^{-1}, respectively. De-occlusion and release of the sugar are electroneutral and proceed with an estimated rate of ~250 s^{-1} (see the text). H^+ release on the cytoplasmic side (red) is the major electrogenic step in the overall transport cycle and characterized by a pH-dependent rate constant (0.3−30 s^{-1}). The observation that sugar occlusion is only weakly electrogenic (6% of the total charge translocated per turnover) is graphically represented by a "shallow" H^+ binding site in $C_{occ}H^+Lac$, while strongly electrogenic H^+ release (94% of the total charge translocated per turnover) is represented by a "deep" H^+ release site in C_{in}.

With MelB, a rapid initial charge translocation initiated by sugar binding is also observed [250 s^{-1} (*22*)], and evidence indicating that sugar displacement across the membrane ($C_{out}H^+Lac \rightarrow C_{in}H^+Lac$) is a two-step process has been presented. It was also proposed that the initial charge displacement corresponds to the formation of an occluded state (*40*). Therefore, in both symporters, evidence that sugar binding leads to the electrogenic formation of an intermediate occluded state is accumulating.

ACKNOWLEDGMENT

We thank Michael Schmalenberg for assistance during the SSM measurements.

REFERENCES

1. Saier, M. H., Jr., Beatty, J. T., Goffeau, A., Harley, K. T., Heijne, W. H., Huang, S. C., Jack, D. L., Jahn, P. S., Lew, K., Liu, J., Pao, S. S., Paulsen, I. T., Tseng, T. T., and Virk, P. S. (1999) The major facilitator superfamily. *J. Mol. Microbiol. Biotechnol. 1*, 257–279.
2. Saier, M. H., Jr. (2000) Families of transmembrane sugar transport proteins. *Mol. Microbiol. 35*, 699–710.
3. Abramson, J., Smirnova, I., Kasho, V., Verner, G., Kaback, H. R., and Iwata, S. (2003) Structure and mechanism of the lactose permease of *Escherichia coli*. *Science 301*, 610–615.
4. Kaback, H. R., Sahin-Toth, M., and Weinglass, A. B. (2001) The kamikaze approach to membrane transport. *Nat. Rev. Mol. Cell Biol. 2*, 610–620.
5. Kaback, H. R. (2005) The Passion of the Permease. In Biophysical and Structural Aspects of Bioenergetics (Wikström, M., Ed.) pp 359−373, Royal Society of Chemistry, Cambridge, U.K.
6. Kaback, H. R. (2005) Structure and mechanism of the lactose permease. *C. R. Biol 328*, 557–567.
7. Guan, L., and Kaback, H. R. (2006) Lessons from lactose permease. *Annu. Rev. Biophys. Biomol. Struct. 35*, 67–91.

8. Kaback, H. R., Dunten, R., Frillingos, S., Venkatesan, P., Kwaw, I., Zhang, W., and Ermolova, N. (2007) Site-directed alkylation and the alternating access model for LacY. *Proc. Natl. Acad. Sci. U.S.A. 104*, 491–494.
9. Nie, Y., Ermolova, N., and Kaback, H. R. (2007) Site-directed Alkylation of LacY: Effect of the Proton Electrochemical Gradient. *J. Mol. Biol. 374*, 356–364.
10. Nie, Y., Sabetfard, F. E., and Kaback, H. R. (2008) The Cys154→Gly mutation in LacY causes constitutive opening of the hydrophilic periplasmic pathway. *J. Mol. Biol. 379*, 695–703.
11. Nie, Y., and Kaback, H. R. (2010) Sugar binding induces the same global conformational change in purified LacY as in the native bacterial membrane. *Proc. Natl. Acad. Sci. U.S.A. 107*, 9903–9908.
12. Majumdar, D. S., Smirnova, I., Kasho, V., Nir, E., Kong, X., Weiss, S., and Kaback, H. R. (2007) Single-molecule FRET reveals sugar-induced conformational dynamics in LacY. *Proc. Natl. Acad. Sci. U.S.A. 104*, 12640–12645.
13. Smirnova, I., Kasho, V., Choe, J. Y., Altenbach, C., Hubbell, W. L., and Kaback, H. R. (2007) Sugar binding induces an outward facing conformation of LacY. *Proc. Natl. Acad. Sci. U.S.A. 104*, 16504–16509.
14. Zhou, Y., Guan, L., Freites, J. A., and Kaback, H. R. (2008) Opening and closing of the periplasmic gate in lactose permease. *Proc. Natl. Acad. Sci. U.S.A. 105*, 3774–3778.
15. Smirnova, I., Kasho, V., Sugihara, J., and Kaback, H. R. (2009) Probing of the rates of alternating access in LacY with Trp fluorescence. *Proc. Natl. Acad. Sci. U.S.A. 106*, 21561–21566.
16. Schultz, P., Garcia-Celma, J.-J., and Fendler, K. (2008) SSM-based electrophysiology. *Methods Enzymol. 46*, 97–103.
17. Garcia-Celma, J. J., Smirnova, I. N., Kaback, H. R., and Fendler, K. (2009) Electrophysiological characterization of LacY. *Proc. Natl. Acad. Sci. U.S.A. 106*, 7373–7378.
18. Viitanen, P., Newman, M. J., Foster, D. L., Wilson, T. H., and Kaback, H. R. (1986) Purification, reconstitution, and characterization of the lac permease of *Escherichia coli*. *Methods Enzymol. 125*, 429–452.
19. Costello, M. J., Escaig, J., Matsushita, K., Viitanen, P. V., Menick, D. R., and Kaback, H. R. (1987) Purified *lac* permease and cytochrome o oxidase are functional as monomers. *J. Biol. Chem. 262*, 17072–17082.
20. Pintschovius, J., Fendler, K., and Bamberg, E. (1999) Charge translocation by the Na^+/K^+-ATPase investigated on solid supported membranes: Cytoplasmic cation binding and release. *Biophys. J. 76*, 827–836.
21. Ganea, C., Pourcher, T., Leblanc, G., and Fendler, K. (2001) Evidence for intraprotein charge transfer during the transport activity of the melibiose permease from *Escherichia coli*. *Biochemistry 40*, 13744–13752.
22. Garcia-Celma, J.-J., Dueck, B., Stein, M., Schleuter, M., Mayer-Lipp, K., Leblanc, G., and Fendler, K. (2008) Rapid activation of the melibiose permease MelB immobilized on a solid-supported membrane. *Langmuir 24*, 8119–81128.
23. Carrasco, N., Antes, L. M., Poonian, M. S., and Kaback, H. R. (1986) *Lac* permease of *Escherichia coli*: Histidine-322 and glutamic acid-325 may be components of a charge-relay system. *Biochemistry 25*, 4486–4488.
24. Carrasco, N., Puttner, I. B., Antes, L. M., Lee, J. A., Larigan, J. D., Lolkema, J. S., Roepe, P. D., and Kaback, H. R. (1989) Characterization of site-directed mutants in the *lac* permease of *Escherichia coli*. 2. Glutamate-325 replacements. *Biochemistry 28*, 2533–2539.
25. Guan, L., and Kaback, H. R. (2004) Binding affinity of lactose permease is not altered by the H^+ electrochemical gradient. *Proc. Natl. Acad. Sci. U.S.A. 101*, 12148–12152.
26. Smirnova, I. N., Kasho, V. N., and Kaback, H. R. (2006) Direct Sugar Binding to LacY Measured by Resonance Energy Transfer. *Biochemistry 45*, 15279–15287.
27. Smirnova, I. N., Kasho, V. N., Sugihara, J., Choe, J. Y., and Kaback, H. R. (2009) Residues in the H^+ translocation site define the pK_a for sugar binding to LacY. *Biochemistry. 48*, 8852–8860.
28. Gropp, T., Cornelius, F., and Fendler, K. (1998) K^+-dependence of electrogenic transport by the NaK-ATPase. *Biochim. Biophys. Acta 1368*, 184–200.
29. Garcia, M. L., Viitanen, P., Foster, D. L., and Kaback, H. R. (1983) Mechanism of lactose translocation in proteoliposomes reconstituted with lac carrier protein purified from *Escherichia coli*. 1. Effect of pH and imposed membrane potential on efflux, exchange, and counterflow. *Biochemistry 22*, 2524–2531.
30. Kaczorowski, G. J., and Kaback, H. R. (1979) Mechanism of lactose translocation in membrane vesicles from *Escherichia coli*. 1. Effect of pH on efflux, exchange, and counterflow. *Biochemistry 18*, 3691–3697.
31. Viitanen, P., Garcia, M. L., Foster, D. L., Kaczorowski, G. J., and Kaback, H. R. (1983) Mechanism of lactose translocation in proteoliposomes reconstituted with lac carrier protein purified from *Escherichia coli*. 2. Deuterium solvent isotope effects. *Biochemistry 22*, 2531–2536.
32. Herzlinger, D., Viitanen, P., Carrasco, N., and Kaback, H. R. (1984) Monoclonal antibodies against the *lac* carrier protein from *Escherichia coli*. 2. Binding studies with membrane vesicles and proteoliposomes reconstituted with purified *lac* carrier protein. *Biochemistry 23*, 3688–3693.
33. Mirza, O., Guan, L., Verner, G., Iwata, S., and Kaback, H. R. (2006) Structural evidence for induced fit and a mechanism for sugar/H^+ symport in LacY. *EMBO J. 25*, 1177–1183.
34. Guan, L., Mirza, O., Verner, G., Iwata, S., and Kaback, H. R. (2007) Structural determination of wild-type lactose permease. *Proc. Natl. Acad. Sci. U.S.A. 104*, 15294–15298.
35. Sahin-Tóth, M., and Kaback, H. R. (2001) Arg-302 facilitates deprotonation of Glu-325 in the transport mechanism of the lactose permease from *Escherichia coli*. *Proc. Natl. Acad. Sci. U.S.A. 98*, 6068–6073.
36. van Iwaarden, P. R., Driessen, A. J., Menick, D. R., Kaback, H. R., and Konings, W. N. (1991) Characterization of purified, reconstituted site-directed cysteine mutants of the lactose permease of *Escherichia coli*. *J. Biol. Chem. 266*, 15688–15692.
37. van Iwaarden, P. R., Driessen, A. J., Lolkema, J. S., Kaback, H. R., and Konings, W. N. (1993) Exchange, efflux, and substrate binding by cysteine mutants of the lactose permease of *Escherichia coli*. *Biochemistry 32*, 5419–5424.
38. Meyer-Lipp, K., Ganea, C., Pourcher, T., Leblanc, G., and Fendler, K. (2004) Sugar Binding Induced Charge Translocation in the Melibiose Permease from *Escherichia coli*. *Biochemistry 43*, 12606–12613.
39. Yousef, M. S., and Guan, L. (2009) A 3D structure model of the melibiose permease of *Escherichia coli* represents a distinctive fold for Na. *Proc. Natl. Acad. Sci. U.S.A. 106*, 15291–15296.
40. Meyer-Lipp, K., Sery, N., Ganea, C., Basquin, C., Fendler, K., and Leblanc, G. (2006) The inner interhelix loop 4−5 of the melibiose permease from *Escherichia coli* takes part in conformational changes after sugar binding. *J. Biol. Chem. 281*, 25882–25892.